Resource

Cell

Rapid, Low-Cost Detection of Zika Virus Using Programmable Biomolecular Components

Graphical Abstract

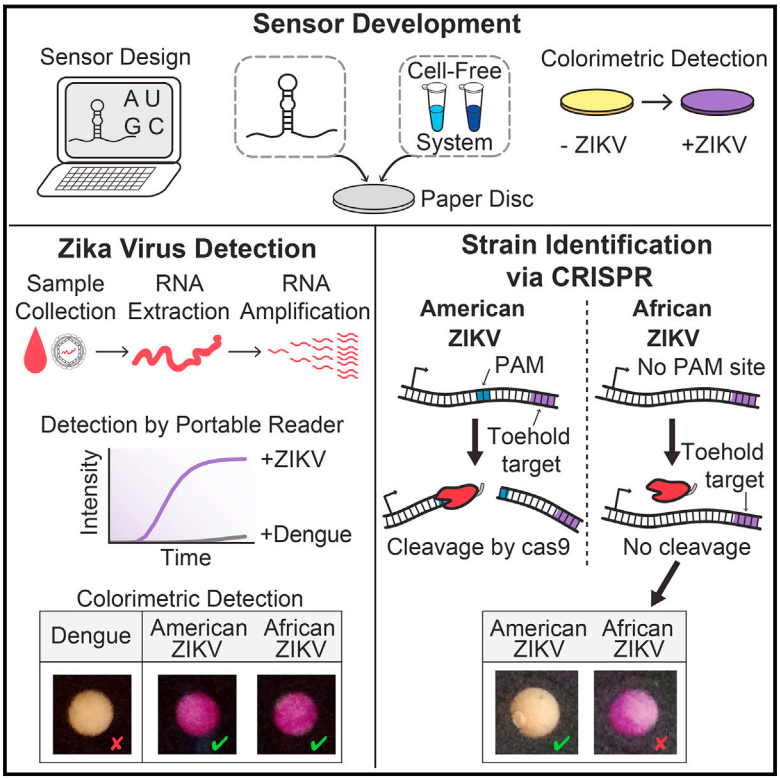

Highlights

- A portable, low-cost diagnostic platform for the detection of Zika virus
- Discrimination of viral strains at single-base resolution using a CRISPR-based tool
- Low femtomolar detection of Zika virus from infected monkey plasma
- Programmable sensor development workflow for rapid responses to global epidemics

Authors

Keith Pardee, Alexander A. Green, Melissa K. Takahashi, ..., David H. O'Connor, Lee Gehrke, James J. Collins

Correspondence

jimjc@mit.edu

In Brief

A diagnostic platform utilizing biomolecular sensors and CRISPR-based technology allows rapid, specific, and low-cost detection of the Zika virus at clinically relevant concentrations.

Pardee et al., 2016, Cell *165*, 1255–1266
May 19, 2016
http://dx.doi.org/10.1016/j.cell.2016.04.059

CellPress

Resource

Cell

Rapid, Low-Cost Detection of Zika Virus Using Programmable Biomolecular Components

Keith Pardee,[1,14] Alexander A. Green,[2,14] Melissa K. Takahashi,[3,14] Dana Braff,[3,4,5,14] Guillaume Lambert,[5,6,14] Jeong Wook Lee,[5] Tom Ferrante,[5] Duo Ma,[2] Nina Donghia,[5] Melina Fan,[7] Nichole M. Daringer,[3] Irene Bosch,[3] Dawn M. Dudley,[8] David H. O'Connor,[8] Lee Gehrke,[3,9,10] and James J. Collins[3,5,10,11,12,13,*]

[1]Leslie Dan Faculty of Pharmacy, University of Toronto, Toronto, ON M5S 3M2, Canada
[2]Biodesign Center for Molecular Design and Biomimetics, The Biodesign Institute and the School of Molecular Sciences, Arizona State University, AZ 85287, USA
[3]Institute for Medical Engineering & Science, Massachusetts Institute of Technology, Cambridge, MA 02139, USA
[4]Department of Biomedical Engineering, Boston University, Boston, MA 02215, USA
[5]Wyss Institute for Biologically Inspired Engineering, Harvard University, Boston, MA 02115, USA
[6]School of Applied and Engineering Physics, Cornell University, Ithaca, NY 14853, USA
[7]Addgene, Cambridge, MA 02139, USA
[8]Wisconsin National Primate Research Center and Department of Pathology and Laboratory Medicine, UW-Madison, Madison, WI 53706, USA
[9]Department of Microbiology and Immunobiology, Harvard Medical School, Boston, MA 02115, USA
[10]Harvard-MIT Program in Health Sciences and Technology, Cambridge, MA 02139, USA
[11]Department of Biological Engineering, Massachusetts Institute of Technology, Cambridge, MA 02139, USA
[12]Synthetic Biology Center, Massachusetts Institute of Technology, Cambridge, MA 02139, USA
[13]Broad Institute of MIT and Harvard, Cambridge, MA 02142, USA
[14]Co-first author
*Correspondence: jimjc@mit.edu
http://dx.doi.org/10.1016/j.cell.2016.04.059

SUMMARY

The recent Zika virus outbreak highlights the need for low-cost diagnostics that can be rapidly developed for distribution and use in pandemic regions. Here, we report a pipeline for the rapid design, assembly, and validation of cell-free, paper-based sensors for the detection of the Zika virus RNA genome. By linking isothermal RNA amplification to toehold switch RNA sensors, we detect clinically relevant concentrations of Zika virus sequences and demonstrate specificity against closely related Dengue virus sequences. When coupled with a novel CRISPR/Cas9-based module, our sensors can discriminate between viral strains with single-base resolution. We successfully demonstrate a simple, field-ready sample-processing workflow and detect Zika virus from the plasma of a viremic macaque. Our freeze-dried biomolecular platform resolves important practical limitations to the deployment of molecular diagnostics in the field and demonstrates how synthetic biology can be used to develop diagnostic tools for confronting global health crises.

INTRODUCTION

The emerging outbreak of Zika virus in the Americas has brought this once obscure pathogen to the forefront of global healthcare. Mostly transmitted by *Aedes aegypti* and *A. albopictus* mosquitoes, Zika virus infections have been further spread by international travel and have expanded to large, heavily populated regions of South, Central, and North America (Bogoch et al., 2016). Correlations between the increase in Zika virus infections, the development of fetal microcephaly (Calvet et al., 2016; Galindo-Fraga et al., 2015; Victora et al., 2016), and Guillain-Barré syndrome have resulted in the declaration of a public health emergency by the World Health Organization (WHO) and a call for fast-tracked development of Zika virus diagnostics (Oehler et al., 2014; Smith and Mackenzie, 2016; WHO, 2016).

Synthetic biology is an emerging discipline that has great potential to respond to such pandemics. The increasing ability of synthetic biologists to repurpose and engineer natural biological components for practical applications has led to new opportunities for molecular diagnostics (Kotula et al., 2014; Lu et al., 2013; Slomovic et al., 2015). We previously developed two biotechnologies that dramatically lower the cost of and technical barriers to the development of synthetic biology-based diagnostics. The first technology, programmable RNA sensors called toehold switches, can be rationally designed to bind and sense virtually any RNA sequence (Green et al., 2014). The second technology, a freeze-dried, paper-based, cell-free protein expression platform, allows for the deployment of these toehold switch sensors outside of a research laboratory by providing a sterile and abiotic method for the storage and distribution of genetic circuits at room temperature (Pardee et al., 2014). We combined these technologies to create a platform for rapidly and inexpensively developing and deploying diagnostic sensors.

In the context of the Zika virus outbreak, the paper-based sensors offer a solution to the critical challenges facing diagnosis of the virus. Standard serological approaches, such as antibody

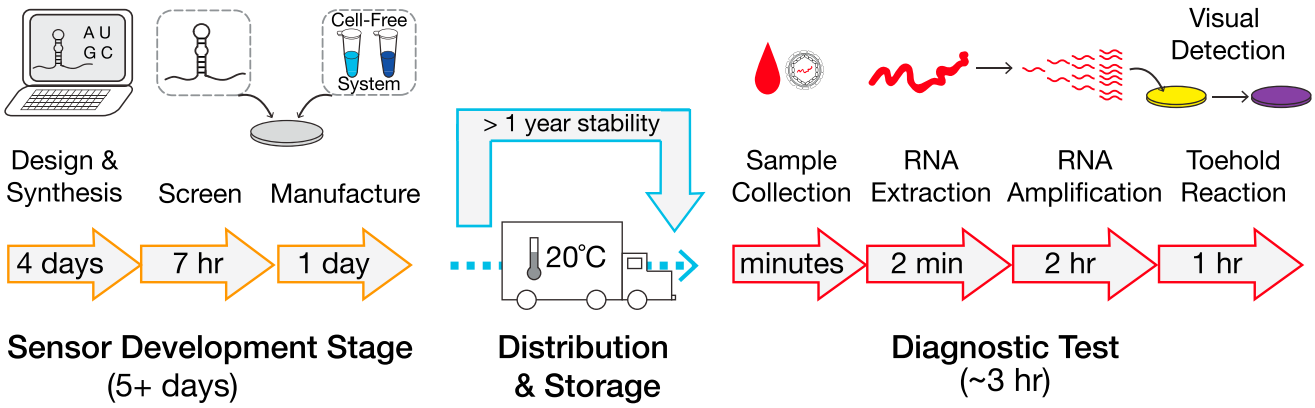

Figure 1. Workflow for the Rapid Prototyping of Paper-Based, Biomolecular Sensors for Portable and Low-Cost Diagnostics

Using sequence information from online databases, primers for isothermal RNA amplification and toehold switch-based RNA sensors were designed in silico using purpose-built algorithms. Once synthesized, the resulting sequence-specific toehold sensors can be assembled and validated in less than 7 hr. In under a day, validated sensors can be embedded into paper and freeze-dried along with a cell-free transcription and translation system to be deployed in the field as stable diagnostics. For the diagnostic test, extracted RNA is isothermally amplified via NASBA and used to rehydrate the freeze-dried paper sensors. The detection of the appropriate trigger RNA is indicated by a color change in the paper disc from yellow to purple.

detection, are limited in diagnostic value due to cross-reactivity in patients that have previously been infected by other flaviviruses circulating in the region. As a result, accurate diagnosis requires nucleic acid-based detection methods, such as PCR and isothermal nucleic acid amplification (Lanciotti et al., 2008; de M Campos et al., 2016; Tappe et al., 2014; Zammarchi et al., 2015). However, such techniques are relatively expensive, require technical expertise to run and interpret, and utilize equipment that is incompatible with use in remote and low-resource locations where surveillance and containment are critically needed.

Here, we demonstrate the rapid development of a diagnostic workflow for sequence-specific detection of Zika virus that can be employed in low-resource settings (Figure 1). We have addressed limitations in the practical deployment of nucleic acid-based molecular diagnostics by combining isothermal RNA amplification with toehold switch sensors on our freeze-dried, paper-based platform. We automate the amplification primer and sensor design process using in silico algorithms and demonstrate a high-throughput pipeline to assemble and test 48 Zika sensors in less than 7 hr. Clinically relevant sensitivity is attained using our amplification and detection scheme, and we report no significant detection of the closely related Dengue virus. To further increase diagnostic capabilities, we develop a CRISPR/Cas9-based module that discriminates between Zika genotypes with single-base resolution. Finally, we employ a simple sample-preparation protocol to reliably extract viral RNA and demonstrate robust detection with this scheme using active Zika virus samples.

RESULTS

In Silico Toehold Switch Design

Toehold switch sensors are programmable synthetic riboregulators that control the translation of a gene via the binding of a *trans*-acting trigger RNA. The switches contain a hairpin structure that blocks gene translation in *cis* by sequestration of the ribosome binding site (RBS) and start codon. Upon a switch binding to a complementary trigger RNA, sequestration of the RBS and start codon is relieved, activating gene translation (Figures 2A and 2B) (Green et al., 2014). To allow for colorimetric detection of trigger RNA sequences, the sensors can be designed to regulate translation of the enzyme LacZ, which mediates a color change by converting a yellow substrate (chlorophenol red-β-D-galactopyranoside) to a purple product (chlorophenol red).

Toehold switch sensors for sequence-based detection of Zika virus were generated using a modified version of the previously developed in silico design algorithm (Supplemental Information) (Green et al., 2014). The modified algorithm screened the genome of the Zika strain prevalent in the Americas (Genbank: KU312312) for regions compatible with RNA amplification and toehold switch activation. The selected Zika genome regions were then computationally filtered to eliminate potential homology to the human transcriptome and to a panel of related viruses, including Dengue and Chikungunya. A total of 24 unique regions of the Zika genome compatible with downstream sensing efforts were identified.

Two toehold switches, each utilizing a different design scheme, were designed for each region, resulting in a total of 48 sensors. The first design scheme, termed the A series, utilizes a modification to the original toehold switch (Green et al., 2014) that reduces the size of the loop domain from 18 nts to 11 nts (Figure 2A) to discourage loop-mediated docking of the ribosome and therefore reduce leakage in the OFF state. The second design scheme, termed the B series, features a 12-nt loop and incorporates a more thermodynamically stable stem in order to lower OFF state gene expression (Figure 2B).

Rapid, In Vitro Sensor Assembly and Screening

In vitro assembly and initial screening of all 48 sensors took place in a 7 hr time period, with low costs associated with sensor development (DNA input $20 USD/sensor) and testing

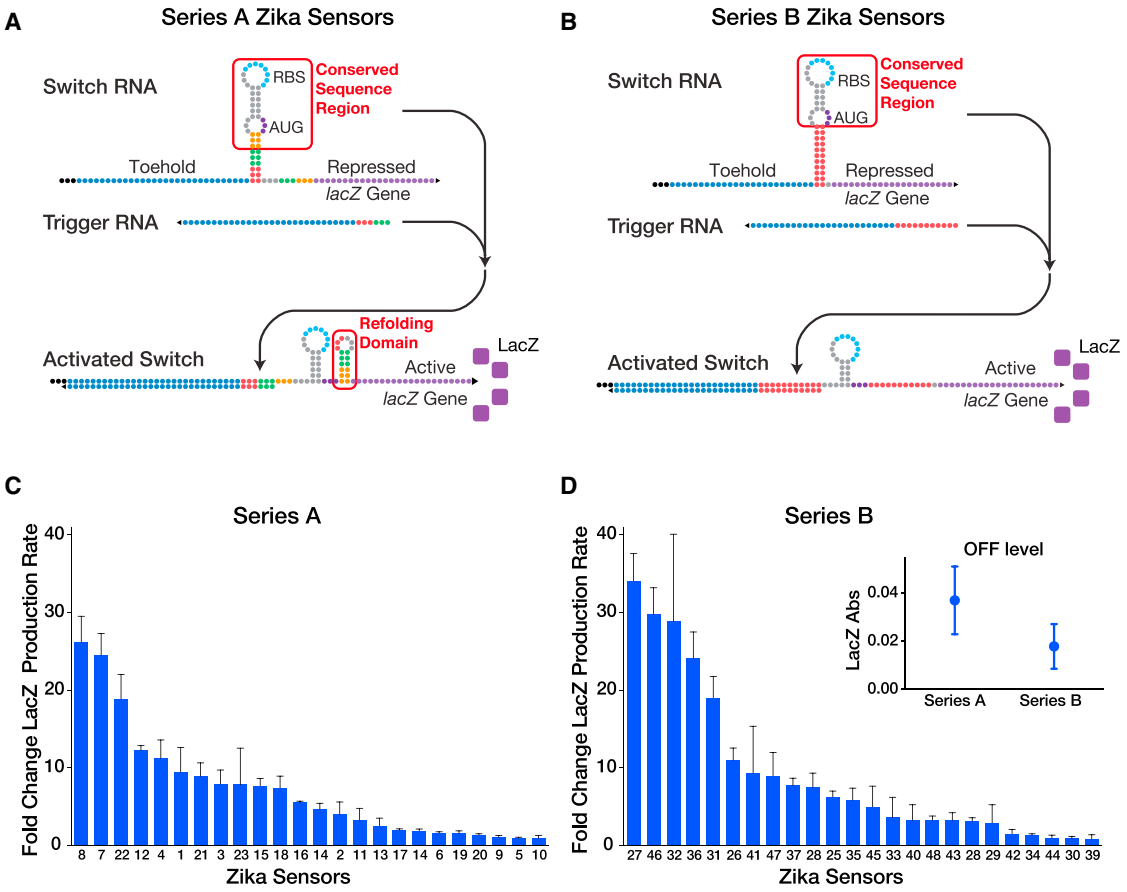

Figure 2. Rapid Prototyping of 48 Paper-Based RNA Toehold Sensors for Zika Virus Detection

(A) Series A toehold switch sensor schematic. The sensor design from Green et al. (2014) was modified with a shortened 11-nt loop sequence to reduce leakage of output gene expression.

(B) Series B toehold switch sensor schematic. Based on the same Zika genomic region as the A series, these sensors include a 12-nt loop and lack the refolding domain. These modifications were made to further reduce LacZ reporter leakage in the OFF state.

(C) Maximum fold change in the rate of LacZ production for the Series A Zika virus RNA sensors during the first 90 min at 37°C. Fold change of LacZ production rate is determined from the slope of absorbance at 570 nm over time (sensor alone versus sensor with 3,000 nM RNA trigger). Sensors are ordered according to fold change.

(D) Maximum fold change in the rate of LacZ production for the Series B Zika virus RNA sensors during the first 90 min at 37°C. Error bars represent SD from three replicates. Inset: average LacZ absorbance of the OFF states at 60 min indicates an overall reduction in LacZ reporter leakage for the Series B sensors. Error bars represent SD across the 24 sensors.

See also Figure S1 and Table S1.

($0.10–$1/test). All 48 sensors and 24 targeted genomic regions were assembled in-house using in vitro protocols. Toehold switches were constructed by ligating the sensors (~130 nt) to a LacZ reporter element in a single 2 hr PCR-based step. Sensor performance screening to assess each sensor against its respective trigger RNA element (Zika genome fragment) was completed using low volume, cell-free transcription and translation reactions on paper. We found that 25 (52%) of the 48 sensors produce a fold change of five or greater in the presence of the appropriate trigger element (128–178 nucleotide regions of the Zika genome; Figures 2C, 2D, and S1). The top-ranked sensors exhibited activation as high as 34-fold over sensor alone (sensor 27B) and were activated in as quickly as 20 min after incubation at 37°C (sensors 7A and 8A). For all sensors, maximum fold change occurred within the first 90 min. Averaging the LacZ output from sensors not exposed to trigger RNA confirmed that the low background design of the series B toehold switch sensors successfully reduced signal leakage (Figure 2D, inset).

Assessing and Improving Zika Sensor Sensitivity

We selected top performing sensors from both the A and B series for trigger RNA titration experiments and found that all chosen sensors were activated with as little as 30 nM of trigger RNA (Figure 3A). The sensors displayed a linear response to RNA concentration, providing semiquantitative information on input trigger RNA values (Figure S2A). Additionally, our top three sensors were highly orthogonal to each other when challenged with a high dose of trigger RNA from off-target Zika sequences (3,000 nM) (Figure S2B).

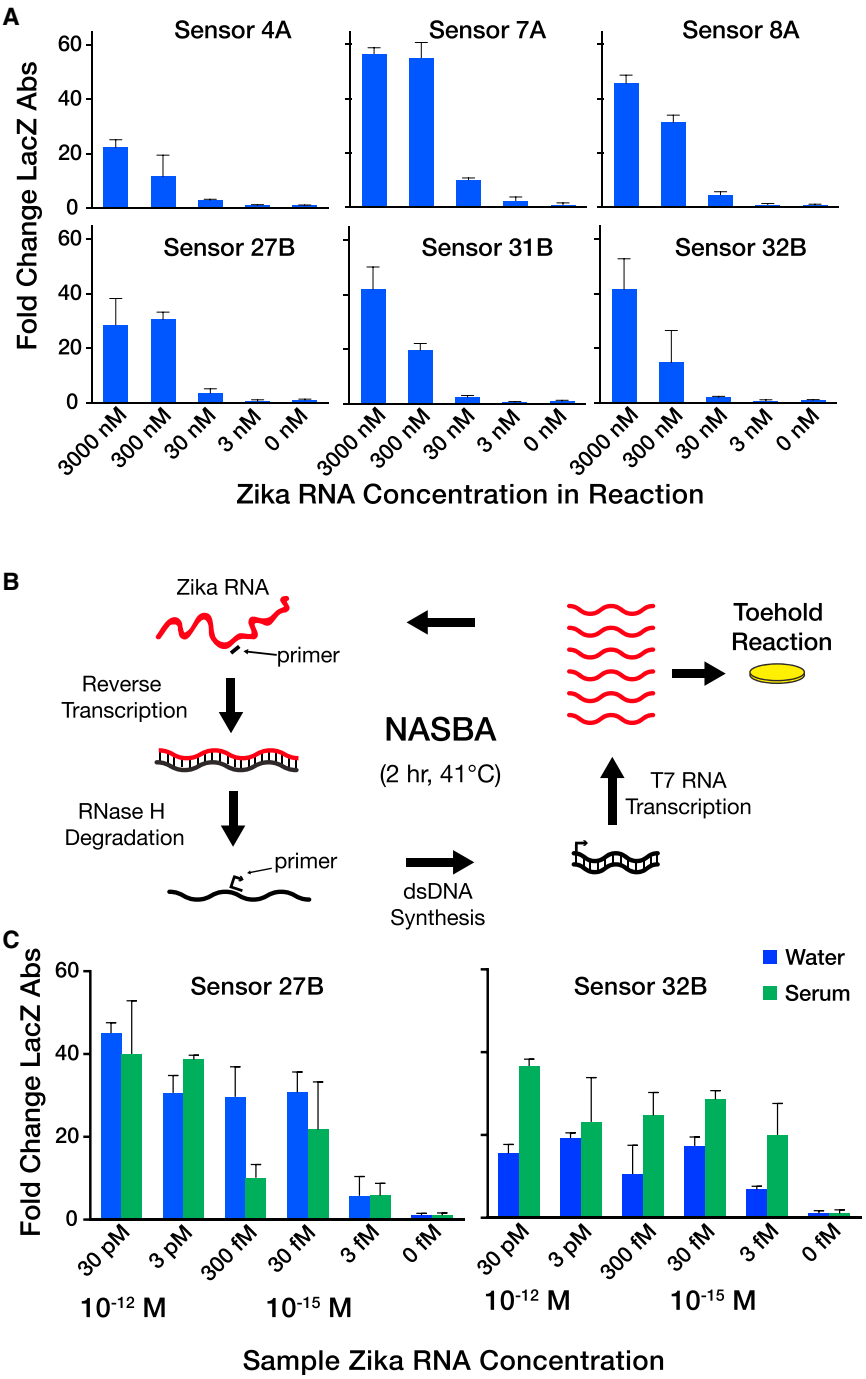

Figure 3. Isothermal RNA Amplification Improves Sensitivity of Toehold Switch Sensors to Allow for Detection of Femtomolar Concentrations of Zika Virus RNA Fragments

(A) Sensitivity of six of the best performing Series A and B sensors without RNA amplification. Fold change is calculated from absorbance (570 nm) after 30 min at 37°C. Error bars represent SD from three replicates.

(B) A schematic of NASBA (nucleic acid sequence based amplification)-mediated RNA amplification.

(C) Zika RNA fragments diluted in water or 7% human serum were amplified using NASBA with input concentrations ranging from 30 pM down to 3 fM. A 1:7 dilution of the NASBA reaction in water was then used to rehydrate freeze-dried, paper-based reactions containing sensors 27B and 32B. Fold change is calculated as described in (A) after 30 min at 37°C.

See also Figure S2 and Table S2.

Though the sensors displayed specificity for their respective Zika RNA trigger, they were unable to detect clinically relevant RNA concentrations. Zika viral loads have been documented as high as 202 × 10^6 copies/ml (365 fM) in urine (Gourinat et al., 2015). However, viral loads in saliva and serum are reportedly even lower, with 3 × 10^6 copies/ml (4.9 fM) (Barzon et al., 2016) documented in patient saliva and 2.5 × 10^6 copies/ml (4.1 fM) (Zika Experimental Science Team, 2016) and 7.2 × 10^5 copies/ml (1.2 fM) (Lanciotti et al., 2008) in primate and patient serum, respectively. Accordingly, to increase the sensitivity of our diagnostic platform, we incorporated an isothermal RNA amplification technique known as NASBA (nucleic acid sequence-based amplification) into our workflow (Figure 1).

NASBA is a promising candidate for use with our diagnostic scheme because it is known to be extremely sensitive and has a proven track record in field-based diagnostic applications (Cordray and Richards-Kortum, 2012). The amplification process begins with reverse transcription of a target RNA that is mediated by a sequence-specific reverse primer to create an RNA/DNA duplex. RNase H then degrades the RNA template, allowing a forward primer containing the T7 promoter to bind and initiate elongation of the complementary strand, generating a double-stranded DNA product. T7-mediated transcription of the DNA template then creates copies of the target RNA sequence. Importantly, each new target RNA can be detected by the toehold switch sensors and also serve as starting material for further amplification cycles. NASBA requires an initial heating step (65°C), followed by isothermal amplification at 41°C (Figure 3B) (Guatelli et al., 1990).

NASBA was performed on trigger RNA corresponding to Zika genomic regions for sensors 27B and 32B. Trigger RNAs were spiked into either water or human serum (7%) to more closely mimic clinical samples. NASBA reactions were run for 2 hr and then applied to freeze-dried, paper-based sensors. We saw detection with Zika sensors from NASBA reactions initiated with as little as 3 fM of trigger RNA (Figure 3C),

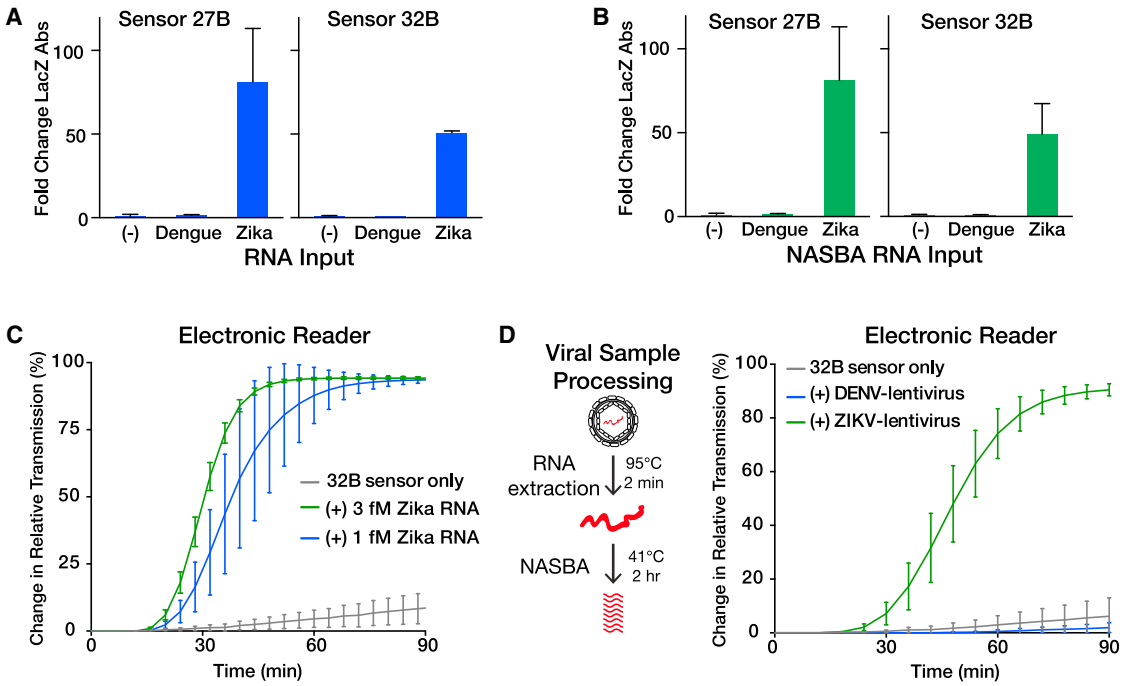

Figure 4. Moving toward a Field-Ready Diagnostic for Zika Virus

(A) Sequence specificity of Zika virus sensors 27B and 32B. Sensors were challenged with 3,000 nM of RNA corresponding to target sequences from the Zika virus or the homologous region of the Dengue virus. Fold change is calculated from absorbance (570 nm) at 60 min after rehydration and incubation of freeze-dried, paper-based reactions at 37°C. Error bars represent SD from three replicates.

(B) Zika virus sensors 27B and 32B were tested for specificity using NASBA reaction products derived from 300 fM input RNA corresponding to target genomic regions of the Zika or Dengue viruses in 7% human serum. Fold change was calculated as in (A).

(C) Using the portable electronic reader, time-course data were collected for Zika virus sensor 32B in the presence of RNA amplified from 1 fM or 3 fM inputs of trigger RNA in 7% human serum. To increase sensitivity, NASBA reactions were run for 2.5 hr. Graphs plot the relative absorbance of 570 nm wavelength light compared to background, which was collected every minute from freeze-dried, cell-free reactions embedded into paper.

(D) Incorporating viral sample processing into the diagnostic workflow. Lentivirus was packaged with Zika RNA or homologous Dengue RNA fragments targeted by sensor 32B. Three femtomolar of virus was spiked into 7% human serum and heated to 95°C for 2 min to extract viral RNA. The boiled lysate was used to initiate NASBA-mediated RNA amplification. A 1:7 dilution of the 2 hr NASBA reaction in water was then used to rehydrate freeze-dried paper-based reactions. Time-course data were collected on the portable electronic reader as in (C).

See also Figure S3.

a value within the range of reported patient viral loads. Zika sensor detection of NASBA-amplified trigger RNA proved to be reliable on samples spiked into either serum or water (Figure S2C). Additionally, for reactions initialized with high concentrations of trigger RNA (> 300 fM), NASBA reaction times could be reduced to as little as 30 min (Figure S2D). NASBA reagents are compatible with freeze-drying (Figure S2E) and could therefore be easily deployed and utilized alongside our paper-based sensors. We also demonstrated that NASBA can be run in the absence of the initial heating step (65°C) (Figure S2F), further reducing the technical and power requirements for deployment.

Moving toward a Field-Ready Diagnostic Platform

To move our experiments toward conditions more representative of those found in clinics worldwide, we focused on three key efforts: (1) testing sensor specificity against related viruses that share clinical symptoms, partial homology, and geographic range with Zika virus; (2) building a second-generation portable, battery-powered reader to provide lab-quality results in low-resource environments; and (3) developing a low-cost and tractable method for viral RNA extraction.

Although our sensor design algorithm screened for Zika genomic sequences that are mostly distinct from those of related viruses, the targeted Zika sequences do share substantial similarity (51%–59%) with their Dengue virus counterparts (Figures S3A and S3B). To test the Zika sensors for possible cross-reactivity, we exposed the sensors to regions of the Dengue genome that share a degree of homology with regions targeted in the Zika genome. Sensors 27B and 32B were treated with high concentrations of RNA amplicons (3,000 nM) from either Zika or Dengue genomic regions. As seen in Figure 4A, Dengue RNA sequences failed to activate the toehold switch sensors. We also tested our NASBA primer sets for specificity to their targeted Zika sequences by applying the NASBA-mediated amplification and paper-based detection scheme to 300 fM inputs of the Dengue and Zika RNA in human serum (7%). Again, we did not see a response to the Dengue RNA sequences, demonstrating robust sequence specificity in our amplification and detection scheme (Figure 4B).

As part of our efforts to advance the paper-based sensor platform toward field-ready diagnostics, we designed a second-generation portable electronic reader to serve as an accessible, low-cost companion technology that provides robust and quantitative measurements of sensor outputs. The electronic reader was assembled using readily available consumer components, open-source code, and laser-cut acrylic housing, with a total cost of just under $250 (Figure S4 and Table S3). The reader is powered by a lithium ion battery (18.5 hr) that can be re-charged via micro USB and houses onboard data storage (4 GB) to resolve the need for an attached laptop during diagnostic reads (Pardee et al., 2014). To achieve sensitive detection of toehold switch signal output, an acrylic chip that holds the freeze-dried, paper-based reactions is placed into the reader between an LED light source (570 nm) and electronic sensors (Figure S4B). Using onboard electronics, each sample is read 29 times per minute, providing low-noise measurements of changes in light transmission due to LacZ-mediated color change.

To demonstrate the utility of the companion reader, we monitored detection of 1 fM and 3 fM of Zika RNA amplicons that had been amplified in NASBA reactions for 2.5 hr. The reader detected significant signal from both samples, which are within the reported range of Zika virus in patient serum (1.2 fM) and urine (365 fM) (Gourinat et al., 2015; Lanciotti et al., 2008), after just over 20 min (Figure 4C).

Our next challenge was to develop a technique to release RNA from the viral capsid using simple methodology compatible with low-resource environments. To this end, we tested the efficacy of boiling viral samples to break down the capsid. For initial development, we engineered lentivirus, which is also an RNA virus, to encapsulate the regions of either the Zika or Dengue genomes that correspond to the sensor 32B target sequence (Figure S3B). These proxy Zika and Dengue viruses were spiked into human serum (7%) at a final concentration of 3 fM and heated to 95°C for either 1 or 2 min. The resulting lysates were then immediately used to initiate NASBA reactions, in order to simulate what might be recovered from a patient sample. Boiling the viral samples for one minute was sufficient to release detectable amounts of RNA in our amplification and toehold switch detection scheme (Figure S3C). NASBA reactions from 2 min boiled samples were also monitored for sensor activation on the portable electronic reader. We detected strong sensor activation in less than 30 min from 3 fM of lentivirus carrying Zika RNA. We were also able to demonstrate clear discrimination between lentiviruses containing Zika and Dengue RNA sequences (Figure 4D).

A NASBA-CRISPR Cleavage Assay to Discriminate between Zika Strains

During epidemic outbreaks, it is often valuable to monitor pathogen lineage and geographic spread. In some cases, genetic variants may be responsible for different clinical manifestations of infection. For example, the Zika strain found in Brazil has been uniquely connected with higher incidences of fetal microcephaly and Guillain-Barré syndrome (Calvet et al., 2016; Mlakar et al., 2016). To allow for strain-specific detection and tracking, we developed an assay that provides single-base discrimination in a manner that is compatible with our freeze-dried sensor platform. Our assay, which we term NASBA-CRISPR Cleavage (NASBACC), leverages the sequence-specific nuclease activity of CRISPR/Cas9 to discriminate between viral lineages (Figure 5A). To do this, NASBACC exploits the ability of Cas9 to selectively cleave DNA only in the presence of an NGG protospacer adjacent motif (PAM). Since any non-biased mutation has a 48% probability of either creating a new PAM site or destroying an existing one (Table S4), there are many strain-specific PAM sites that can be used for lineage discrimination (Figures 5B and 5C). In the NASBACC detection scheme, RNA sequences undergo NASBA amplification utilizing a reverse primer designed to append the trigger sequence of a synthetic toehold switch (sensor H, Figure 5A) (Pardee et al., 2014). In the presence of the appropriate PAM sequence and guide RNA target site, the double-stranded DNA that is synthesized as part of the NASBA reaction undergoes Cas9-mediated cleavage, resulting in a truncated RNA product that is unable to activate the sensor H toehold switch. In the absence of the PAM sequence, the full-length RNA product containing the sensor H trigger sequence is generated, allowing for sensor H activation. Trigger RNA is only amplified from DNA that is not cut by Cas9, thereby allowing for strain-specific detection using toehold sensor H.

Using the paper-based system, sensor 32B was able to distinguish between Zika and Dengue RNA sequences. However, this sensor could not discriminate between the African (GenBank: KF268950) and American (GenBank: KU312312) Zika variants (Figure 5D), a feature that may be useful in certain diagnostic applications. To address this, we applied our NASBACC detection scheme to discriminate between the African and American Zika strains. Due to a single-base difference in the trigger regions of these two strains, a PAM site only exists in the American-lineage sequence (Figure 5C). Thus, only the American strain sequence was cleaved by Cas9, which led to amplification of truncated RNA that did not activate the sensor H toehold switch (Figure 5E). Conversely, the African strain sequence does not contain the PAM site and was not cleaved by Cas9, which resulted in amplification of full-length RNA that activated the sensor H toehold switch. Incorporating NASBACC into our diagnostic workflow can provide precise genotypic information within a few hours. As with the other biomolecular elements of this workflow, Cas9 is compatible with lyophilization and could be used in the field (Figure S5).

Diagnostic Workflow Validation with Active Zika Virus

We next sought to validate our sensor platform with live Zika virus. First, we verified that our amplification and detection scheme could successfully detect full-length genomic RNA purified from Zika virus (Uganda strain MR 766) (Figure 6A). We designed new NASBA primers to accommodate sequence differences between the Uganda Zika strain (GenBank: AY632535) and the American Zika strain (GenBank: KU312312) that our sensors and primers had originally been designed to detect. Computational analysis suggested that Uganda-lineage Zika RNA would activate sensor 32B despite two base mismatches in the toehold region, and this was confirmed experimentally (Figure 6A). We also demonstrated sensor orthogonality to full-length genomic Dengue RNA isolated from three different Dengue serotypes using these methods (Figure 6A).

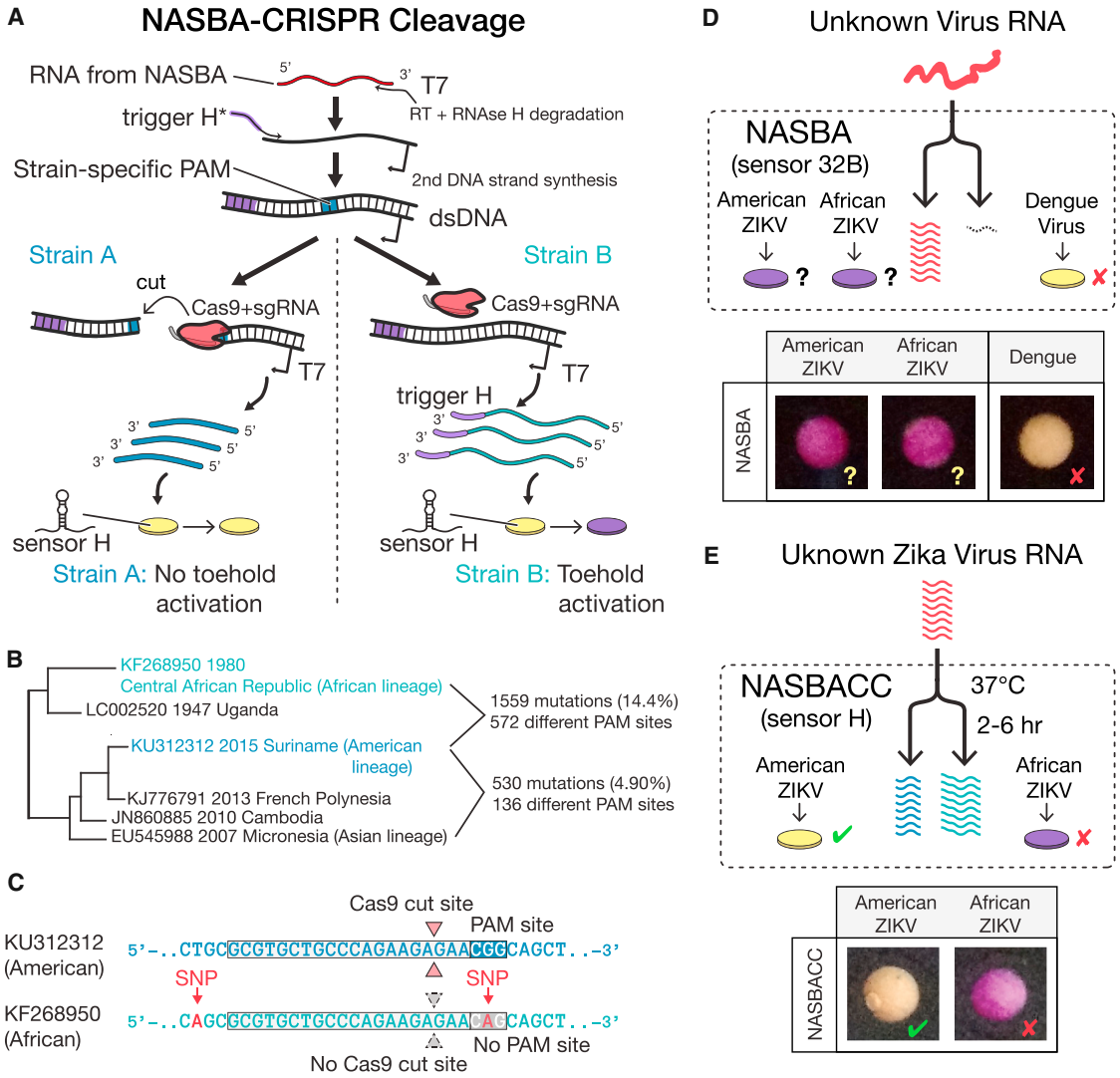

Figure 5. NASBA-CRISPR Cleavage (NASBACC) Allows for Strain Differentiation at Single-Base Resolution

(A) Schematic representation of NASBACC genotyping following a positive Zika diagnosis. A synthetic trigger sequence is appended to a NASBA-amplified RNA fragment through reverse transcription. The presence of a strain-specific PAM leads to the production of either truncated or full-length trigger RNA, which differentially activates a toehold switch (sensor H) (Pardee et al., 2014).

(B) The probability that a non-biased single nucleotide polymorphism (SNP) between two strains can be discriminated by CRISPR/Cas9 is 48% (Table S4). Hence, genetic drift between the American and African or Asian strains, while relatively small (14.4% and 4.9% sequence dissimilarity, respectively), has created hundreds of strain-specific PAM sites.

(C) A SNP between African (GenBank: KF268950) and American (GenBank: KU312312) strains at site 7330 disrupts an existing PAM site, allowing for Cas9-mediated DNA cleavage only in the American strain.

(D) Sensor 32B can distinguish between Dengue and Zika RNA sequences but cannot discriminate between American and African Zika strains. Paper discs containing sensor 32B were rehydrated with 300 nM trigger RNA corresponding to sequences from American-Zika, African-Zika, or Dengue. Colorimetric outputs: a purple color indicates the activation of LacZ expression from the toehold switch, and a yellow color indicates the toehold switch remained inactive.

(E) NASBACC can discriminate between American- and African-lineages of Zika virus. Paper discs containing sensor H were rehydrated with a 1:10 dilution of NASBACC reactions initiated with 0.05 μl of a 300 nM RNA sample. In this case, an inactive toehold switch leads to a positive identification of the American Zika strain.

Once we confirmed that the sensors behaved as expected on full-length genomic RNA, we sought to validate the sample preparation scheme and diagnostic workflow from start to finish. Active Zika virus was cultured in the laboratory and spiked into human serum (7%) at a final concentration of 10 fM, to mimic a clinical sample. The viral sample was then heated to 95°C for 2 min, and the resulting lysate was subjected to NASBA amplification for three hours. Sensor activation from the NASBA-amplified viral sample was monitored on the portable electronic reader. We successfully detected activation of sensor 32B from a diagnostic workflow initiated with live Zika virus (Figure 6B).

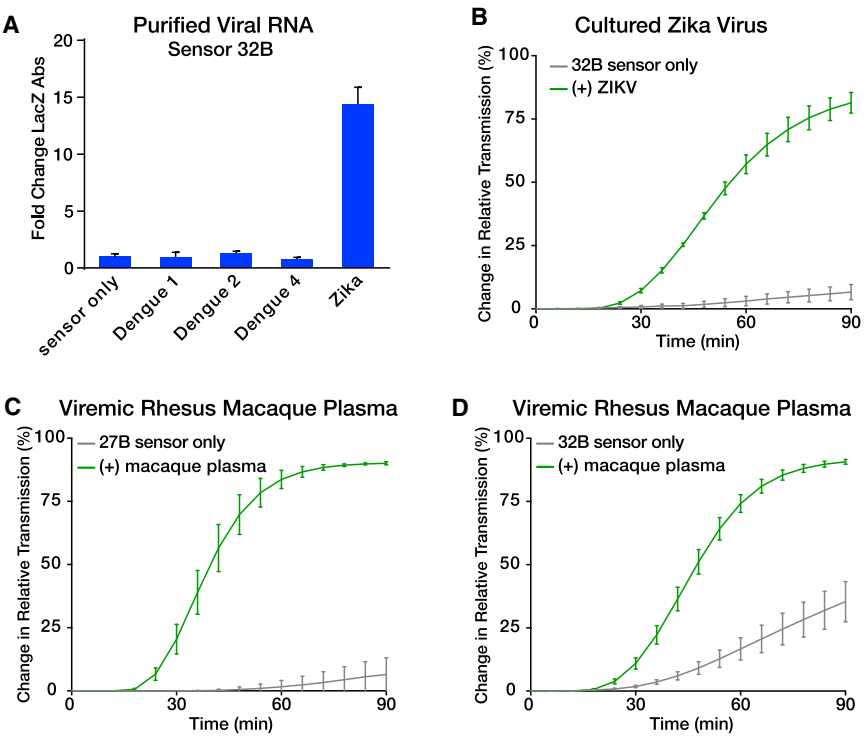

Figure 6. Validation of Diagnostic Workflow on Live Zika Virus Samples

(A) Specificity of sensor 32B against purified genomic RNA. Sensor 32B was tested for specificity using NASBA reaction products performed on 30 fM RNA purified from Zika virus and three different Dengue virus serotypes. Fold change is calculated from absorbance (570 nm) at 60 min after rehydration and incubation of freeze-dried, paper-based reactions at 37°C. Error bars represent SD from three replicates.

(B) Detection of live Zika virus. Ten femtomolar of laboratory-cultured Zika virus was spiked into human serum (7%), heated to 95°C for 2 min, and used to initiate NASBA-mediated RNA amplification. A 1:7 dilution of the 3 hr NASBA reaction in water was then used to rehydrate freeze-dried, paper-based reactions. Time-course data were collected on the portable electronic reader. Graph plots the relative absorbance of 570 nm wavelength light compared to background. Error bars represent SD from three replicates.

(C and D) Detection of Zika virus in viremic rhesus macaque plasma using sensors 27B and 32B. Plasma containing 2.8 fM of Zika virus was diluted 1:10 in nuclease free water, heated to 95°C for 2 min, and used to initiate NASBA-mediated RNA amplification. 3 hr NASBA reactions were monitored on the portable electronic reader as in (B).

For the final validation of our system, we acquired and tested plasma samples from a viremic macaque infected with Zika virus (GenBank: KJ776791) (Zika Experimental Science Team, 2016). The macaque was found to have a plasma viral load of 1.7×10^6 copies/ml (2.8 fM) by a standard qRT-PCR protocol, which was within the detection limits of our platform as tested on synthetic RNA amplicons (Figure 4C). The viremic plasma was diluted 1:10 in water to reduce known inhibitory effects of plasma on downstream reactions and was then taken through our sample processing and diagnostic workflow. The sample was heated to 95°C for 2 min and then amplified via NASBA for 3 hr. Paper-based reactions were monitored on the portable electronic reader and showed strong activation with both sensors 27B and 32B in less than 30 min (Figures 6C and 6D).

DISCUSSION

Rapid Sensor Development Pipeline for Low-Resource Molecular Diagnostics

We have devised a rapid diagnostic development pipeline in response to the ongoing Zika virus outbreak. The serious but poorly understood complications of this viral infection make its timely diagnosis critical for patient health and for limiting its rapid proliferation. However, the poor performance of antibody detection methods (Lanciotti et al., 2008; de M Campos et al., 2016; Tappe et al., 2014; Zammarchi et al., 2015) and the limitations of traditional sequence-based diagnostics have left technical and economic challenges to meeting diagnostic needs.

Our paper-based platform directly addresses these needs by enabling sequence-specific detection of Zika virus in a low-cost manner that is tractable in low-resource settings. By freeze-drying cell-free transcription and translation systems with genetic sensors onto paper, we have created a sterile and abiotic platform that can be utilized outside of laboratory conditions without concern over biosafety. Furthermore, the freeze-dried biomolecular components remain stable at room temperature, allowing for easy storage and distribution in global settings. Our application is easy to use, relying on a colorimetric output that can be read by the naked eye or with a low-cost, battery-operated companion reader, and we are actively working to improve field-readiness via development of a third-generation reader with onboard capabilities for sample preparation and incubation.

The streamlined sensor development platform we describe here provides a generalizable method for a rapid response to any emerging outbreak. Our automated design process computationally screens for sequence specificity and feeds into a high-throughput protocol for rapid sensor prototyping in vitro. We augmented our diagnostic sensors with an upstream target-amplification scheme that allows for detection of target sequences in the low femtomolar range, bringing sensor sensitivity in line with in-patient virus concentrations (Gourinat et al., 2015; Lanciotti et al., 2008). Additionally, we demonstrated that simply boiling an RNA virus liberates sufficient material for downstream amplification and detection processes (Figures 4D, 6, and S3C), and we developed a CRISPR-based tool for accurate strain genotyping on paper (Figure 5). Finally, our methods were validated on viremic plasma samples (Figures 6C and 6D), demonstrating a level of sensitivity that would be required for use of this diagnostic scheme in the field.

Isothermal RNA Amplification and Nucleic-Acid-Based Diagnostics for Low-Resource Settings

Our unique approach of linking NASBA to a downstream synthetic gene network for output detection can be applied to any nucleic acid amplification scheme. This innovative development addresses several key technical and economic challenges in the employment of isothermal amplification methods in the field. Namely, although NASBA has exceptional sensitivity to low-level infections, the technique is costly ($5–$20/test) and susceptible to contamination that can lead to off-target products and false positives (Casper et al., 2007; Cordray and Richards-Kortum, 2012; Ulrich et al., 2010). Our diagnostic scheme addresses both of these points and brings NASBA closer toward application in low-resource settings. The low-volume paper-based reactions only use a fraction of a microliter of NASBA product ($0.51/μl), significantly reducing the total cost of NASBA per test. Additionally, linking NASBA to a synthetic gene network for signal detection allows for rapid and sensitive output reads in a cost-effective manner ($0.10–$1/test) that is practical for use in low-resource settings. Furthermore, the chance for false-positive results due to contamination is minimized by the use of sequence-specific toehold switch sensors and CRISPR/Cas9-mediated selection downstream of the amplification. Our ability to eliminate the initial 65°C heating step (Figure S2F) traditionally used in NASBA reactions streamlines the diagnostic protocol for in-field use and reduces the requirements of the hardware necessary for monitoring results. Finally, we have shown that NASBA reagents can be freeze-dried (Figure S2E) and therefore could be distributed around the world at room temperature alongside our toehold switch sensors. We are also actively working toward combining NASBA and toehold switch sensor reactions in a one-pot assay that will further streamline the diagnostic protocol and shorten the timeframe for readout.

We note that certain components within blood are known to inhibit PCR (Schrader et al., 2012) and similarly affect all nucleic acid based diagnostics, including NASBA. However, we found that a simple dilution of serum or plasma into water sufficiently removes this effect in our diagnostic scheme. We therefore used diluted human serum (7%) as a matrix for our exploratory experiments and diluted viremic plasma samples (10%) for our final validation experiment. The dilution step does affect the overall sensitivity of the diagnostic platform, but we have shown that increasing the NASBA reaction time can sufficiently compensate for reduced sensitivity. Indeed, we were able to detect 2.8 fM of Zika virus from plasma samples from an infected rhesus macaque using our dilution protocol (Figures 6C and 6D). Additionally, a recent study found that Zika virus can be detected at high concentrations in saliva (Barzon et al., 2016), which may not inhibit nucleic acid amplification to the same extent as blood. We are actively working to test other clinical matrices for compatibility with our diagnostic platform.

A Robust and Field-Ready Sample Preparation Scheme for RNA Viruses

In this work, we implemented a simple procedure to extract viral RNA that does not require specialized laboratory equipment. By simply boiling (95°C) virus samples for 2 min, we were able to extract sufficient quantities of RNA for amplification and detection in our diagnostic platform (Figures 4D and 6B–6D). We note that we worked quickly to transfer boiled viral samples to NASBA reactions that contained RNase inhibitors to protect the integrity of the viral RNA. In practice, other commercially available reagents could be added to the sample to protect the RNA from degradation upon collection. Of note, we were able to reliably extract RNA from three different sample types using our methodology: engineered lentivirus (Figure 4D), cultured Zika virus (Figure 6B), and plasma from an infected rhesus macaque (Figures 6C and 6D), highlighting the robustness of our sample preparation scheme.

Programmability of Molecular Sensors Can Address Rapidly Changing Diagnostic Needs

Our platform provides multiple levels of molecular programmability that greatly improve diagnostic specificity. Both the toehold switches and NASBA primers can be designed to target regions specific to a given genome, while excluding regions with significant homology to other organisms. We demonstrated the effectiveness of this design algorithm with sensor 32B, which was able to distinguish genomic Zika RNA from the genomic RNA of three different Dengue serotypes (Figure 6A). Additionally, the NASBACC module allows for single-base discrimination and can be rationally designed to distinguish between different genotypes, adding to the overall programmability of our platform (Figure 5E). Given the high sensor success rate and low barriers to development, we envision that sensors could be easily multiplexed to ensure high-confidence diagnosis (reducing both false negative and false positive results) while keeping costs low. Furthermore, the diagnostic platform could be deployed as panels that include sensors for strain-specific identification and related infections to help monitor the spread of illness.

However, in some cases, it is beneficial for a diagnostic platform to be able to tolerate genetic mutations within a particular nucleic acid sequence. Evolutionary drift, for example, is an unavoidable feature of our ongoing arms race with pathogens that all molecular diagnostics must confront. Our assay in particular has the capacity to tolerate the expected genetic variation found in nature. We analyzed the binding between the toehold switch 32B and RNA sequences from homologous regions in Zika strains isolated from Africa and Asia (Supplemental Information: Supplemental Experimental Procedures). Both of these strains are predicted to fully activate the toehold sensors, even with up to 4-nt (11%) mismatches. In fact, we were able to demonstrate this using RNA triggers from the American strain, two different African strains, and an Asian-lineage of the virus (Figures 5D and 6). Additionally, a critical feature of our technology is the ability to rapidly and inexpensively prototype new genetic sensors, thus allowing for a rapid response to genetic variations and mutations as they arise.

Freeze-Dried Biomolecular Networks for Addressing Real-World Issues in Real Time

With our goal of responding to the ongoing outbreak in a timely manner, we began our work using synthetic RNA fragments spiked into human serum, followed by engineered lentiviruses to mimic clinical samples. As with many proof-of-concept diagnostic studies, synthetic samples provided us with a powerful

tool for optimizing our sensor platform ahead of the regulatory demands required for use of live pathogens (Antunes et al., 2015; Crannell et al., 2014; Rohrman et al., 2012; Stefan et al., 2016; Yen et al., 2015). Through collaborative efforts with the Zika virus community, we were able to test our platform on live Zika virus and were pleased to find similar detection thresholds with Zika virus isolated from infected Vero cells (Figure 6B) and plasma samples from an infected rhesus macaque (Figures 6C and 6D). Our rapid response to the ongoing Zika virus outbreak and our ability to achieve clinically relevant sensitivity and specificity highlight the utility and practicality of this platform technology.

Our synthetic biology pipeline for rapid sensor design and prototyping could be applied to a broad range of public health threats, allowing for rapid development of new diagnostics when and where they are most needed. The ease of in vitro sensor synthesis will allow for the widespread use of validated sensor sequences, aiding rapid global responses to current and future health crises. Finally, our ability to expeditiously design and implement our biomolecular diagnostics for an emerging pathogen using the engineering principles of synthetic biology suggests that the field will play an ever-increasing role in the support and improvement of human health.

EXPERIMENTAL PROCEDURES

In Silico Sensor Design and DNA Synthesis

A set of 48 toehold switch sensors and corresponding NASBA primers were generated using an integrated in silico design algorithm. See the Supplemental Experimental Procedures section in the Supplemental Information for details.

DNA Sensor Assembly

Toehold switch constructs were amplified from DNA templates (Integrated DNA Technologies) and ligated to the *lacZ* reporter gene via PCR. Plasmids were constructed for characterization of the top six toehold switches (Figure 3A). The DNA templates were amplified using PCR and inserted into pET system parent plasmids (EMD Millipore) using Gibson assembly (Gibson et al., 2009) with 30 bp overlap regions. Plasmids for sensors 27B and 32B are available through Addgene (plasmid numbers: 75006–75011).

Cell-Free Reactions

Details of RNA sensor validation are described in Pardee et al. (2014). Briefly, amplified sensor DNA was column purified and tested on paper discs (2 mm) containing freeze-dried, cell-free reactions (NEB, PURExpress) in the presence or absence of trigger RNA coding for a complementary region of the Zika virus genome (128–178 nts). The cell-free reactions consisted of: NEB Solution A (40%) and B (30%), chlorophenol red-β-D-galactopyranoside (Sigma, 0.6 mg/ml), RNase inhibitor (Roche, 03335402001; 0.5%), and linear DNA constructs encoding the toehold sensors (0.33 nM). The paper discs (Whatman, 1442-042) were blocked in 5% BSA overnight prior to use. Trigger RNA was produced using T7 RNAP-based transcription (Epicenter ASF3257) from linear DNA templates. Paper-based reactions (1.8 μl) were incubated at 37°C using either our companion electronic reader inside a humidified chamber or a plate reader (BioTek Neo). For the in-house reader, paper discs were placed into 2 mm holes in a removable acrylic chip; for the plate reader, paper discs were placed into black, clear bottom 384-well plates (Corning 3544).

NASBA

For NASBA reactions, the trigger elements (128–178 nts) were extended by 100 nts on the 5′ and 3′ ends with the relevant Zika genome sequence to provide suitable template RNAs. RNA amplicons were spiked into 7% human serum (Sigma H4522) where indicated. Reaction Buffer (Life Sciences NECB-24; 33.5%), Nucleotide Mix (Life Sciences NECN-24; 16.5%), RNase inhibitor (Roche, 03335402001; 0.5%), 12.5 μM of each NASBA primer (2%), nuclease free water (2.5%), and RNA amplicon (20%) were assembled at 4°C and incubated at 65°C for 2 min, followed by a 10 min incubation at 41°C. Enzyme Mix (Life Sciences NEC-1-24; 25%) was then added to the reaction (for a final volume of 5 μL), and the mixture was incubated at 41°C for 2 hr unless noted otherwise. For output reads with paper-based toeholds, the NASBA reactions were diluted 1:7 in water. See Table S2 for primer sequences.

Lentivirus Preparation and Processing

HEK293FT cells (Life Technologies, R70007) used for virus packaging were cultured in DMEM supplemented with 10% FBS, 1% penicillin-streptomycin, and 4 mM GlutaMAX (ThermoFisher Scientific). 12 hr prior to transfection, 6.5×10^6 cells were seeded in a 10 cm dish. 7.5 μg psPAX2, 2.5 μg pMD2.G, and 10 μg pSB700 modified to include a Zika or Dengue RNA fragment were transfected using the HeBS-$CaCl_2$ method. Media was changed 12 hr post-transfection. 27 hr after changing media, viral supernatant was harvested and filtered using a 0.45 μm syringe filter. Viral supernatant was then purified with ViraBind Lentivirus Purification Kit (Cell Biolabs VPK-104) and buffer exchanged into 1xPBS with Lenti-X Concentrator (Clontech, 631231). Viral RNA concentration was quantified using QuickTiter Lentivirus Quantification Kit (VPK-112). Virus samples were spiked into 7% human serum at a final volume of 25 μl. Samples were heated to 95°C for 1 and 2 min and used as input to NASBA.

Zika Virus Preparation and Processing

100 μl of Zika virus isolate (MR 766) was utilized for infection of 10^6 Vero cells in 4 ml of media (DMEM supplemented with 2% fetal calf serum [FCS] and penicillin-streptomycin). The supernatant was removed after 2 hr of incubation at 37°C and replaced with fresh media (DMEM, 10% FCS) for 48 hr of infection. Cell debris was removed by centrifugation at 1,500 rcf for 10 min, and aliquots of the virus were stored at −80°C until use. The virus was buffer exchanged into 1xPBS with Lenti-X Concentrator (Clontech, 631231). Viral RNA concentrations were determined from virus purified with the QIAamp Viral RNA Mini Kit (QIAGEN 52904) and confirmed with qRT-PCR. The titer of the Zika virus used was 6.7×10^7 infectious units per milliliter (Lambeth et al., 2005). Virus samples were spiked into 7% human serum at a final volume of 30 μl. Samples were heated to 95°C for 2 min and used as input to NASBA. NASBA primers were re-designed to accommodate the MR 766 strain sequence (see Supplemental Information).

Dengue Orthogonality

Genomic RNA from three Dengue serotypes was purified using the QIAamp Viral RNA Mini Kit (QIAGEN 52904). Dengue 1 (GenBank: KM204119), Dengue 2 (GenBank: KM204118), Dengue 4 (GenBank: AF326573). NASBA reactions using the sensor 32B primer set were performed on 30 pM RNA for 2 hr. NASBA reactions were diluted 1:7 in water and used to rehydrate freeze-dried, paper-based reactions containing sensor 32B.

Electronic Optical Reader

The portable device consists of four layers housed within a laser-cut acrylic box fastened together with metal screws and mounting brackets (Figure S4; McMaster-Carr, 8505K14, 98164A061; Digi-Key, 36-621-ND). The top layer holds a multiplexer (Sparkfun, BOB-09056), solderable breadboard (Sparkfun, PRT-12702), friction lock connectors (Digi-Key, A31001-ND, A19473-ND) and 16 LEDs (Digi-Key, 754-1262-ND). The LEDs have a very narrow viewing angle and an emission of 570 nm to match the absorbance maximum of the chlorophenol red product from the LacZ reaction. The LEDs were placed in close proximity to the chip in the middle layer, which holds 16 paper disks within 2 mm apertures. The apertures prevented transmission of stray light and were coaxial with the LEDs in the top layer and the array of 16 TSL2591 sensors (Adafruit, 1980) in the third layer below, which also contained two solderable breadboards and connectors as above. The bottom layer contains the Arduino Uno with an attached Power Shield (Adafruit, 2708) connected to a rechargeable 2,000 mAh lithium ion battery (Adafruit, 2011) on which a data-logging shield (Adafruit, 1141) was stacked with connectors (Digi-Key, A30954-ND, A19476) and a 4GB SD/MicroSD Card (Adafruit, 102). To prevent crosstalk between reads, reactions were read in series by sequentially activating each LED and sensor pair. The read frequency and pattern of the reader

can be easily adjusted by modifying and uploading alternative sketches to the Arduino. The raw data (which is the median of 29 100 ms, 428× gain reads per minute) was saved to the SD card along with the date and time of the run, integration time and gain settings. The data were processed with the MATLAB script and graphed in Prism. A diagram of the circuit and an overview of the laser cut parts can be found in the supplemental figures (Figure S4) and laser cutting patterns, the Arduino sketch and MATLAB script are in Data S1.

Calculation of Fold Change

The calculation of fold change for plate reader data was done by first subtracting the background absorbance measured from paper-based reactions that did not contain sensor DNA or trigger RNA. These normalized values were smoothed to reduce measurement noise using a three-point average of the time point and the data collected 10 min before and after. The minimum value of each well was then adjusted to zero. For data presented in Figures 3, 4, and 6, fold change was calculated from these zero adjusted values by dividing the wells at each time point by the average signal from the corresponding sensor-alone control wells. For our initial sensor screen (Figure 2), we used a more sensitive measure of fold change based on the difference in the rate of color change between control and RNA trigger wells. This was done by calculating the rate of change in normalized absorbance (570 nm) values using slope; where, at each 10 min time point, the rate was calculated using $S_n = (T_{n+1} - T_n)/10$, where T is the normalized data at a time point (T_n) and the time point 10 min later (T_{n+1}), and S_n is the slope reported for T_n. Fold change was then calculated as above. MATLAB script to analyze data collected on a plate reader is provided in Data S1.

NASBA-CRISPR Cleavage (NASBACC)

Reactions were performed in a 5 μl volume containing (NASBA buffer), 1 μl of a 250 nM Cas9 nuclease (NEB, M0386), and 250 nM purified gRNA (GeneArt precision gRNA synthesis kit, ThermoFisher Scientific, A29377) mix, 3 nM NASBACC primers, and 0.4 units of RNase inhibitor (NEB, M0314). The forward NASBACC primer is composed of the reverse complement of the trigger H sequence (5′- GTT TGA ATG AAT TGT AGG CTT GTT ATA GTT ATG TTT-3′) and the forward binding sequence of the (region 32) NASBA primers. The reverse NASBACC primer contains the T7 promoter sequence (5′-CTA ATA CGA CTC ACT ATA GG-3′) followed by the reverse binding sequence of the (region 32) NASBA primers. The assembled reaction was incubated at 37°C for 2–6 hr. For toehold activation assay on freeze-dried paper, NASBACC reactions were diluted 1:10 in nuclease-free water.

Viremic Plasma Processing

Details on macaque care and infection can be found in the Supplemental Experimental Procedures. For processing, plasma was diluted 1:10 in nuclease free water, heated to 95°C for 2 min, and immediately added to a NASBA reaction. NASBA was run for 3 hr.

qRT-PCR to Determine Macaque Plasma Viral Loads

Viral RNA was extracted from 300 μl of plasma using the Viral Total Nucleic Acid Purification Kit (Promega) on a Maxwell 16 MDx instrument. Viral RNA was quantified by qRT-PCR using the primers and probe designed by Lanciotti et al. (2008). The RT-PCR was performed using the SuperScript III Platinum one-step quantitative RT-PCR system (Invitrogen) on the LightCycler 480 instrument (Roche Diagnostics). Primers and probe were used at final concentrations of 600 nm and 100 nm, respectively, along with 150 ng random primers (Promega). Cycling conditions were as follows: 37°C for 15 min, 50°C for 30 min, and 95°C for 2 min, followed by 50 cycles of 95°C for 15 s and 60°C for 1 min. Virus concentration was determined by interpolation onto an internal standard curve composed of seven 10-fold serial dilutions of a synthetic ZIKV RNA fragment based on the Asian lineage.

SUPPLEMENTAL INFORMATION

Supplemental Information includes Supplemental Experimental Procedures, five figures, four tables, and one data file and can be found with this article online at http://dx.doi.org/10.1016/j.cell.2016.04.059.

AUTHOR CONTRIBUTIONS

K.P. designed and performed experiments and co-wrote the manuscript. A.A.G. conceived the low-leakage toehold switches, developed the combined toehold switch and NASBA primer design algorithm, supervised sensor construction, and co-wrote the manuscript. M.K.T and D.B. designed and performed experiments and co-wrote the manuscript. G.L. developed and performed experiments for the NASBACC module and co-wrote the manuscript. J.W.L. performed the portable electronic reader experiments and edited the manuscript. T.F. designed and built the portable electronic reader and edited the manuscript. D.M. developed the rapid sensor assembly procedure and constructed sensor plasmids. N.D. performed experiments and edited the manuscript. M.F. developed the NASBA protocol. N.M.D. cultured the lentivirus samples. I.B. cultured the Zika virus samples. D.M.D. and D.H.O. provided macaque plasma samples and edited the manuscript. L.G. provided the Zika virus samples and edited the manuscript. J.J.C. designed experiments and edited the manuscript.

ACKNOWLEDGMENTS

We would like to thank Marcelle Tuttle from the Church Lab (Wyss Institute) for the vectors used to produce the lentivirus. We would also like to thank Xiao Tan and Shimyn Slomovic for helpful comments on the manuscript, as well as Ewen Cameron, Andres Cubillos, James Niemi and Dionna Williams for assistance with project logistics. The work was supported by the Wyss Institute for Biologically Inspired Engineering, MIT's Center for Microbiome Informatics and Therapeutics, and the Defense Threat Reduction Agency grant HDTRA1-14-1-0006. A.A.G acknowledges startup funds provided by Arizona State University. L.G. acknowledges support from NIH AI100190.

Received: March 15, 2016
Revised: April 19, 2016
Accepted: April 24, 2016
Published: May 6, 2016

REFERENCES

Antunes, P., Watterson, D., Parmvi, M., Burger, R., Boisen, A., Young, P., Cooper, M.A., Hansen, M.F., Ranzoni, A., and Donolato, M. (2015). Quantification of NS1 dengue biomarker in serum via optomagnetic nanocluster detection. Sci. Rep. *5*, 16145.

Barzon, L., Pacenti, M., Berto, A., Sinigaglia, A., Franchin, E., Lavezzo, E., Brugnaro, P., and Palù, G. (2016). Isolation of infectious Zika virus from saliva and prolonged viral RNA shedding in a traveller returning from the Dominican Republic to Italy, January 2016. Euro Surveill. *21*, 30159.

Bogoch, I.I., Brady, O.J., Kraemer, M.U.G., German, M., Creatore, M.I., Kulkarni, M.A., Brownstein, J.S., Mekaru, S.R., Hay, S.I., Groot, E., et al. (2016). Anticipating the international spread of Zika virus from Brazil. Lancet *387*, 335–336.

Calvet, G., Aguiar, R.S., Melo, A.S.O., Sampaio, S.A., de Filippis, I., Fabri, A., Araujo, E.S.M., de Sequeira, P.C., de Mendonça, M.C.L., de Oliveira, L., et al. (2016). Detection and sequencing of Zika virus from amniotic fluid of fetuses with microcephaly in Brazil: a case study. Lancet Infect. Dis. Published online February 17, 2016. http://dx.doi.org/10.1016/S1473-3099(16)00095-5.

Casper, E.T., Patterson, S.S., Bhanushali, P., Farmer, A., Smith, M., Fries, D.P., and Paul, J.H. (2007). A handheld NASBA analyzer for the field detection and quantification of Karenia brevis. Harmful Algae *6*, 112–118.

Cordray, M.S., and Richards-Kortum, R.R. (2012). Emerging nucleic acid-based tests for point-of-care detection of malaria. Am. J. Trop. Med. Hyg. *87*, 223–230.

Crannell, Z.A., Rohrman, B., and Richards-Kortum, R. (2014). Equipment-free incubation of recombinase polymerase amplification reactions using body heat. PLoS ONE *9*, e112146.

de M Campos, R., Cirne-Santos, C., Meira, G.L., Santos, L.L., de Meneses, M.D., Friedrich, J., Jansen, S., Ribeiro, M.S., da Cruz, I.C., Schmidt-Chanasit,

J., and Ferreira, D.F. (2016). Prolonged detection of Zika virus RNA in urine samples during the ongoing Zika virus epidemic in Brazil. J. Clin. Virol. *77*, 69–70.

Galindo-Fraga, A., Ochoa-Hein, E., Sifuentes-Osornio, J., and Ruiz-Palacios, G. (2015). Zika virus: A new epidemic on our doorstep. Rev. Invest. Clín. *67*, 329–332.

Gibson, D.G., Young, L., Chuang, R.-Y., Venter, J.C., Hutchison, C.A., 3rd, and Smith, H.O. (2009). Enzymatic assembly of DNA molecules up to several hundred kilobases. Nat. Methods *6*, 343–345.

Gourinat, A.-C., O'Connor, O., Calvez, E., Goarant, C., and Dupont-Rouzeyrol, M. (2015). Detection of Zika virus in urine. Emerg. Infect. Dis. *21*, 84–86.

Green, A.A., Silver, P.A., Collins, J.J., and Yin, P. (2014). Toehold switches: de-novo-designed regulators of gene expression. Cell *159*, 925–939.

Guatelli, J.C., Whitfield, K.M., Kwoh, D.Y., Barringer, K.J., Richman, D.D., and Gingeras, T.R. (1990). Isothermal, in vitro amplification of nucleic acids by a multienzyme reaction modeled after retroviral replication. Proc. Natl. Acad. Sci. USA *87*, 1874–1878.

Kotula, J.W., Kerns, S.J., Shaket, L.A., Siraj, L., Collins, J.J., Way, J.C., and Silver, P.A. (2014). Programmable bacteria detect and record an environmental signal in the mammalian gut. Proc. Natl. Acad. Sci. USA *111*, 4838–4843.

Lambeth, C.R., White, L.J., Johnston, R.E., and de Silva, A.M. (2005). Flow cytometry-based assay for titrating dengue virus. J. Clin. Microbiol. *43*, 3267–3272.

Lanciotti, R.S., Kosoy, O.L., Laven, J.J., Velez, J.O., Lambert, A.J., Johnson, A.J., Stanfield, S.M., and Duffy, M.R. (2008). Genetic and serologic properties of Zika virus associated with an epidemic, Yap State, Micronesia, 2007. Emerg. Infect. Dis. *14*, 1232–1239.

Lu, T.K., Bowers, J., and Koeris, M.S. (2013). Advancing bacteriophage-based microbial diagnostics with synthetic biology. Trends Biotechnol. *31*, 325–327.

Mlakar, J., Korva, M., Tul, N., Popović, M., Poljšak-Prijatelj, M., Mraz, J., Kolenc, M., Resman Rus, K., Vesnaver Vipotnik, T., Fabjan Vodušek, V., et al. (2016). Zika Virus Associated with Microcephaly. N. Engl. J. Med. *374*, 951–958.

Oehler, E., Watrin, L., Larre, P., Leparc-Goffart, I., Lastere, S., Valour, F., Baudouin, L., Mallet, H., Musso, D., and Ghawche, F. (2014). Zika virus infection complicated by Guillain-Barre syndrome–case report, French Polynesia, December 2013. Euro Surveill. *19*, 20720.

Pardee, K., Green, A.A., Ferrante, T., Cameron, D.E., DaleyKeyser, A., Yin, P., and Collins, J.J. (2014). Paper-based synthetic gene networks. Cell *159*, 940–954.

Rohrman, B.A., Leautaud, V., Molyneux, E., and Richards-Kortum, R.R. (2012). A lateral flow assay for quantitative detection of amplified HIV-1 RNA. PLoS ONE *7*, e45611.

Schrader, C., Schielke, A., Ellerbroek, L., and Johne, R. (2012). PCR inhibitors - occurrence, properties and removal. J. Appl. Microbiol. *113*, 1014–1026.

Slomovic, S., Pardee, K., and Collins, J.J. (2015). Synthetic biology devices for in vitro and in vivo diagnostics. Proc. Natl. Acad. Sci. USA *112*, 14429–14435.

Smith, D.W., and Mackenzie, J. (2016). Zika virus and Guillain-Barré syndrome: another viral cause to add to the list. Lancet *387*, 1486–1488.

Stefan, C.P., Chase, K., Coyne, S., Kulesh, D.A., Minogue, T.D., and Koehler, J.W. (2016). Development of real-time reverse transcriptase qPCR assays for the detection of Punta Toro virus and Pichinde virus. Virol. J. *13*, 54.

Tappe, D., Rissland, J., Gabriel, M., Emmerich, P., Gunther, S., Held, G., Smola, S., and Schmidt-Chanasit, J. (2014). First case of laboratory-confirmed Zika virus infection imported into Europe, November 2013. Euro Surveill. *19*, 20685.

Ulrich, R.M., Casper, E.T., Campbell, L., Richardson, B., Heil, C.A., and Paul, J.H. (2010). Detection and quantification of Karenia mikimotoi using real-time nucleic acid sequence-based amplification with internal control RNA (IC-NASBA). Harmful Algae *9*, 116–122.

Victora, C.G., Schuler-Faccini, L., Matijasevich, A., Ribeiro, E., Pessoa, A., and Barros, F.C. (2016). Microcephaly in Brazil: how to interpret reported numbers? Lancet *387*, 621–624.

WHO (2016). WHO to fast-track availability of diagnostics for Zika virus. http://www.who.int/medicines/news/fast_track_diagnostics_zika/en/.

Yen, C.-W., de Puig, H., Tam, J.O., Gómez-Márquez, J., Bosch, I., Hamad-Schifferli, K., and Gehrke, L. (2015). Multicolored silver nanoparticles for multiplexed disease diagnostics: distinguishing dengue, yellow fever, and Ebola viruses. Lab Chip *15*, 1638–1641.

Zammarchi, L., Stella, G., Mantella, A., Bartolozzi, D., Tappe, D., Günther, S., Oestereich, L., Cadar, D., Muñoz-Fontela, C., Bartoloni, A., and Schmidt-Chanasit, J. (2015). Zika virus infections imported to Italy: clinical, immunological and virological findings, and public health implications. J. Clin. Virol. *63*, 32–35.

Zika Experimental Science Team. (2016). ZIKV-001: Infection of three rhesus macaques with French Polynesian Zika virus. https://zika.labkey.com/project/OConnor/ZIKV-001/begin.view. 2016.